HIGH TEMPERATURE CHEMISTRY - ITS ROLE IN METAL PRODUCTION

P. Grieveson

Department of Metallurgy, Royal School of Mines, Prince Consort Road,
London, S.W.7 2BP, England.

Abstract - An attempt is made to demonstrate the importance of physico-
chemical principles in the extraction and refining of metals. Examples
are taken from ferrous extraction metallurgy and the application of physi-
cal chemistry to the understanding of the various production processes is
demonstrated.

The efficiency of the blast furnace is considered in terms of stoichiometry
and heat balances and slag-metal reactions in the hearth of the furnace
are dealt with in terms of thermodynamics. The kinetics of iron oxide
reduction are discussed with regard to both the blast furnace and the
newer direct reduction processes.

Reactions occurring in oxygen steel-working processes are also considered,
especially variations in reaction path with the top and bottom blown
processes.

Finally the importance of deoxidation and desulphurisation reactions in
the ladle to produce quality metal is discussed.

INTRODUCTION

The reduction and smelting of iron ore is done mainly in the iron blast furnace. The burden
charged at the top of the furnace consists primarily of iron ore, flux and coke. The reducing
gas carbon monoxide and the heat required for the smelting of the ore are generated at the
bottom of the furnace by blowing preheated air into the coke bed. The slag and metal
accumulate as two liquid layers at the bottom of the furnace.

The hot metal produced by the blast furnace is charged to a steelmaking converter with
scrap steel and limestone. Oxygen is blown into the metal bath to decarburise the metal to
the required level usually 0.02 to 0.2%. The steel produced is then deoxidised to the desired
level and cast to give a solid product.

This presentation attempts to illustrate the importance of physico-chemical principles in the
production of metals by looking at a few aspects of iron and steel production. In particular
the importance of mass and heat balances, thermodynamics and kinetics will be shown.

STOICHIOMETRY AND HEAT BALANCE OF THE IRON BLAST FURNACE

An iron blast furnace is a complex piece of equipment in which we have counter-current heat
and mass transfer between gases and burden and wide temperature and oxygen potential varia-
tion. Thus the furnace is a very efficient countercurrent heat exchanger and at the same time
a complex chemical exchange reactor converting iron oxide to iron.

In order that efficient conversion occurs of reactants to products there is an overall chemi-
cal stoichiometry which must be met. In addition, specific thermal requirements must also be
satisfied to permit the endothermic reactions to proceed and the products brought to their
final temperatures. Perhaps the most convenient and simplest representation for both of
these requirements is the use of a WILD diagram. Such a diagram has been constructed in
Figure 1 for a typical iron blast furnace. The vertical scale represents the heat require-
ment in calories and the horizontal one represents the stoichiometric carbon requirement in
gms per two gm atoms of iron (one mole of Fe_2O_3).

At the bottom left of the diagram as a negative thermal quantity, the heat required for the
reaction at 298° of

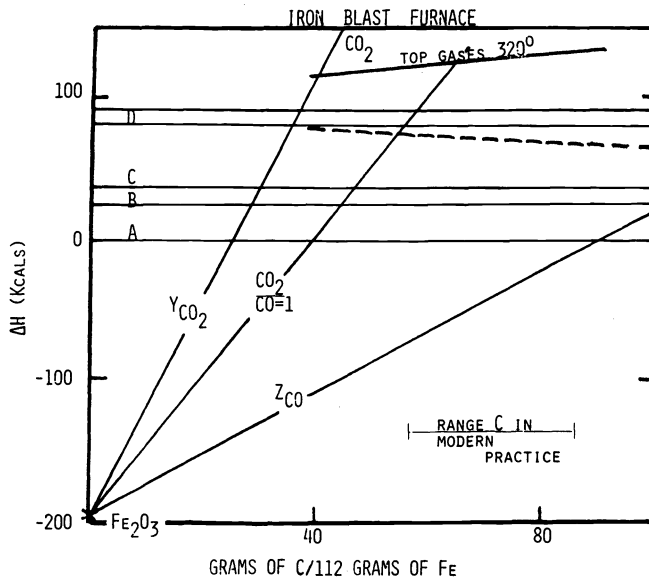$$Fe_2O_3 = 2Fe + {}^3/_2 O_2 \qquad\qquad (1)$$

Fig. 1. Wild diagram of variation of enthalpy change with carbon-iron
ratio for an iron blast furnace.

is plotted as point X. Relative to this point are plotted at Y and Z the heats liberated
when $3/2\ O_2$ is reacted (a) with 18 gm of carbon to produce CO_2 and (b) with 36 gm of C to
give CO. The lines which join these points to X and are extrapolated across the diagram give
the excess or deficit of heat obtained from the combustion of carbon to CO_2 and CO, by the
oxygen released from the ore and by further added oxygen (from the blast). Between these two
lines can be generated a whole family of lines for various CO/CO_2 combustion mixtures. In
this case only that for $CO/CO_2=1$ is produced, as being typical of the top gas composition of a
modern blast furnace.

In the blast furnace, it is necessary to provide additional heat to melt the metal, form and
melt the slag and reduce the various metalloids; Si, P, Mn into the metal, to meet heat
losses and to heat the gases which leave the furnace. The relevant thermal quantities are
plotted above the zero as follows:-

    A - heat to produce Fe at 1400°C.
    B - heat required to reduce 1%Si, 1%P, 1%Mn.
    C - heat to produce 1 tonne slag/tonne of metal.
    D - heat losses.

in each case these are represented by horizontal lines. In addition, we have an upward
sloping line for the gas $N_2 + CO + CO_2$ at the ratio $CO/CO_2 = 1$ and temperature of 320°C,
remembering that the volume of gas increases as the carbon utilisation increases .

From the sum of these heats must be deducted the heat entering with the blast and the line
resulting from this deduction for CO/CO_2 mixture = 1 and preheated blast at 660°C is shown as
the dashed line.

The quantity of carbon required for this set of conditions in a blast furnace is given by the
point where the dashed line and the line representing a gas composition 1:1 intersect - a
coke rate of 480kg/tonne of iron.

The WILD diagram allows an accurate assessment to be made of coke rate for any set of operating
conditions. It demonstrates markedly the advantage of operating the furnace at a high CO_2
content in the exit gas, the advantage to be gained from preheating the blast and the thermal
penalty which is paid for producing large quantities of slags.

As useful as the WILD diagram is in assessing the overall performance of the furnace, it does
not give us any indication as to the temperatures or positions in the furnace where particular
reactions occur. Thus the Reichardt (Ref. 1) diagram which in principle describes the heat
balance over the whole temperature can be more informative. This diagram is shown in its
simplest form in Figure 2 and describes the heat balance in the furnace and is based on the
application of the first and second laws of thermo dynamics. The diagram represents a plot of
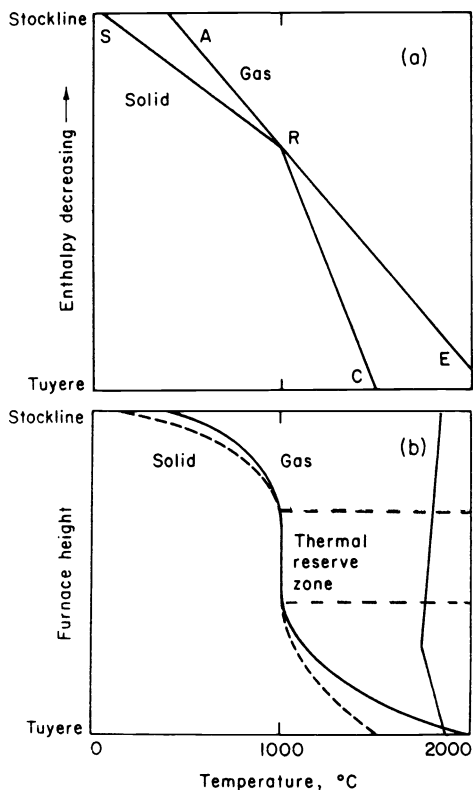
Fig. 2.   Simplified sketch of Reichardt diagram. Variation of enthalpy change
with temperature and temperature profile.

enthalpy of the gases and the burden against temperature along the stack. As a result of
heat transfer, the enthalpy of the gas decreases with decreasing temperature of the ascending
gas, as represented by the line ERA. The increase in the enthalpy of the solids with increa-
sing temperature during descent in the stack is represented by the line SR. In the lower
part of the furnace, the heat capacity of the burden increases because of fusion, the onset
of the endothermic reaction of CO_2 with C to produce CO and greater heat losses; hence the
slope of line RC is greater than that of SR. The net result is that as shown in Figure 2 the
temperature difference between the ascending gas and descending burden reaches a minimum
known as the thermal pinch point.

Depending on the type of burden and blast furnace practice, the temperature level of the
thermal reserve zone can vary from about 900 to 1650°C and the length of the zone can vary
from 1 to 4 m. When the burden contains carbonates, additional pinch points can occur at
temperatures below 900°C where the endothermic dissociation of the carbonate occurs.

Rist (Ref. 2 & 3) has carried out detailed investigations of reduction reactions by simula-
ting the conditions in the stack, and developed a method of graphical representation of heat
and mass balances. For an idealised simple case the number of oxygen atoms per atom of iron
involved in the reaction, O/Fe, is plotted in Figure 3 against the number of oxygen atoms per
mole of gas, O/C. Since the oxidation of CO to CO_2 occurs without any change in the total
number of moles of gas, the oxygen balance is represented by a straight line. The origin of
the co-ordinates is chosen such that the oxygen associated with iron oxide appears on the
positive side of the ordinate, and oxygen in the air blast and in other oxides reduced
(MnO, SiO_2) per gm atom of iron on the negative side of the ordinate. Rist calls the line
AE the optimum operating line from which AB represents indirect reduction of iron oxides by
CO,.BC direct reduction of wustite by carbon, UO reduction of non-ferrous oxides and fusion
and UE combustion in the tuyere zone.

The hatched area outlines the stability region of the iron oxides at the temperature of the
thermal reserve zone. The line passing through point W, representing iron-wustite equili-
brium, is for maximum oxygen exchange for a given top gas composition A, producing the
chemical pinch point in the thermal reserve zone. For wustite to be reduced to iron, the
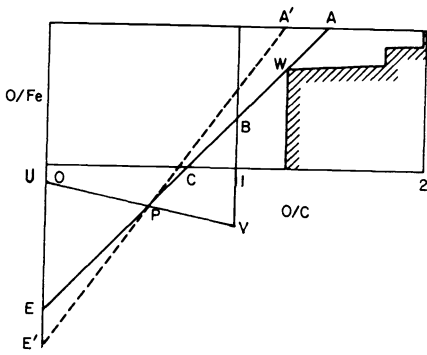line AB must lie above the pinch point W.

Fig. 3. Rist diagram showing the construction of the stoichiometric
        operating line of a blast furnace.

For given conditions of operation, the position of the point P is fixed as a pivot point for
the operating line. The co-ordinates of point P are related to the thermal balance of the
furnace such that X_p is a function of the blast characteristics only (T and composition) and
Y_p is a function of hot metal composition and the heat requirements below the thermal
reserve zone per unit of iron.

The application of the combination of Reichardt - Rist diagrams are ideal for optimising the
operating variables in the blast furnace to achieve low coke rates and high production rates.
In addition, they allow the prediction of the various changes which will occur in furnace
operation.

An illustration of the utility of these diagrams is now given on the effect of an increase
in blast temperature on furnace operation see Figure 4.

An increase in blast temperature means a decrease in the thermal demand of the blast hence a
decrease in blast volume as indicated by the movement of E to E' on the Rist diagram.
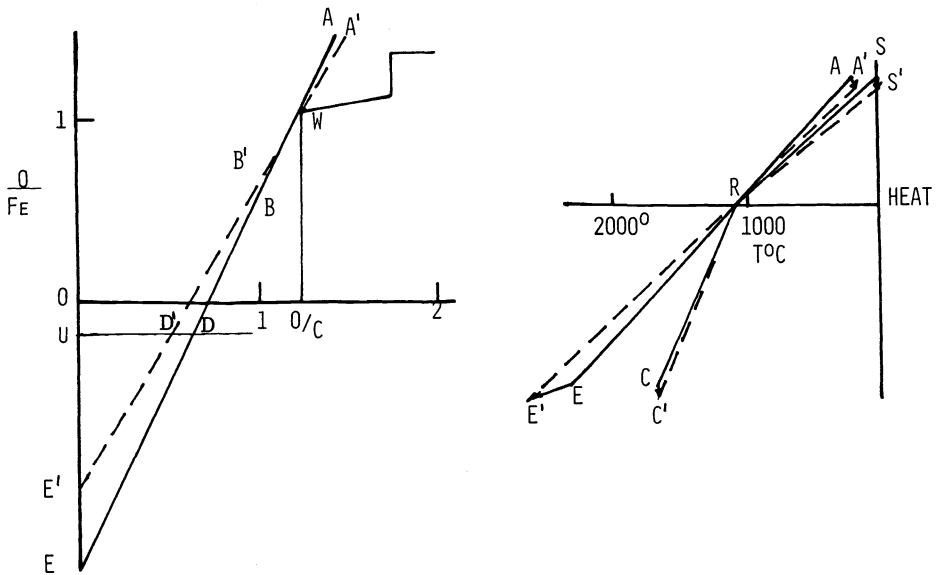

Fig. 4. Simultaneous representation of Rist and Reichardt diagrams:- effect
        of an increase in blast temperature.

The resulting modifications appearing on the diagram are:

    (a) a decrease in slope of the operating line, corresponding to a decrease in coke rate;

    (b) an increase B-B' in the amount of solution loss reaction, both as gas generated and heat required;

    (c) an increase A-A' of the degree of oxidation of the top gas;

    (d) a decrease in the N_2/reducing gas ratio, proportional to D-D':

Corresponding modifications are required in the Reichardt diagram. For ideal heat exchange, the gas line ARE and the segments of the solid lines all hinge on point R which remains fixed. The following changes occur:-

    (i) a decrease in slope for the gas line due to decrease in volume of gas;

    (ii) an increase in heat requirement of the lower zone of the Shaft due to BB' = CC' = vertical component EE';

    (iii) an increase in the virtual flame temperature equal to the horizontal component of EE';

    (iv) a small decrease in heat requirements of the upper zone due to lowering of the coke rate equal to SS' or vertical component of AA';

    (v) a decrease in top gas temperature equal to the horizontal component AA'·

In the Reichardt diagram the decrease in slope of the gas line is the major effect. As a consequence the new angle A'RS' is smaller than the initial one ARS. This indicates that the difference in temperature between the gas and the solid is decreased and heat transfer is slower. The new temperature profile is thus less favourable to fast reduction than the original and the chemical reserve zone will tend to shrink.

The important effect is related to production rate it should be noted that if production rate is maintained constant, the blowing rate must be decreased in the ratio UE' to UE on the Reichardt diagram.

If the blowing rate is maintained constant, production will increase in the ratio UE to UE'.

REDUCTION OF IRON OXIDES

The reactions of primary concern in the iron blast furnaces are the reduction reactions of iron oxides. These reactions have been studied by many workers and the results are well documented in a text by Von Bogdandy and Engell (Ref. 4).

The formation of product layers during the reduction of iron ore is well known. The greater the driving force for reduction and the faster the rate of chemical reaction, the more pronounced is the formation of the product layers. The kinetics of the formation and dissociation of both H_2O and CO_2 on surfaces of dense iron and wustite have been measured by several techniques. There is general agreement that the reaction is first order relative to the partial pressure of the reacting gas

$$FeO + H_2 = Fe + H_2O \tag{2}$$

$$FeO + CO = Fe + CO_2 \tag{3}$$

The following equations can be derived from the experimental data for the temperature dependence of the rate of formation in mole cm^{-2} sec^{-1} atm^{-1} of H_2O from H_2 and CO_2 from CO on the surfaces of iron and wustite (Ref. 5).

For H_2 on iron surfaces

$$\log k_{H_2} = -\frac{4540}{T} + 1.02 \tag{4}$$

For H_2 on wustite surfaces

$$\log k_{H_2} = -\frac{4820}{T} + 2.08 \tag{5}$$

For CO on iron surface

$$\log k_{CO} = -\frac{8770}{T} + 1.27 \tag{6}$$

For CO on wustite surface

$$\log k_{CO} = -\frac{8770}{T} + 0.29 \tag{7}$$

In both cases, the rate of reaction on an iron surface is about an order of magnitude greater than that on wustite.

In the reduction of dense ores or sintered pellets concentric layers of porous magnetite, wustite and iron are formed around the haematite core of the particle. When the thickness of the iron layer reaches 1 to 1.5 mm, the subsequent reduction is controlled primarily by gas diffusion through the pores of the iron layer. If there is no volume change during reduction, the isothermal reduction rate of a spherical particle is given by

$$3 - 2F - 3(1-F)^{2/3} = \frac{6De}{\rho r_o^2} \frac{p_i - (p_i)_e}{RT} t + \text{constant} \tag{8}$$

where F is the Fraction of oxygen removed, r_o is the particle radius, De effective gas diffusivity, p_i the partial pressure of reacting gas in the gas mixture, $(p_i)_e$ equilibrium pressure of the reacting gas.

The interpretation of the initial rate of reduction of large Fe_2O_3 particles are more complex. It has been assumed that the initial rate of reduction is controlled jointly by the partial gas diffusion and the chemical reaction in the pore mouths near the surface of the particle. Under these circumstances the initial rate of reduction may be represented by (Ref. 6).

$$\left(\frac{dF}{dt}\right)_o = \frac{3}{r_o} \left(\frac{S'RTk_{H_2}De}{\rho}\right)^{\frac{1}{2}} (1 + \frac{1}{K})^{\frac{1}{2}} \frac{p^o_{H_2} - P/1+K}{RT} \tag{9}$$

where K is the equilibrium constant $(p_{H_2O} / p_{H_2})_e$ for co-existing iron and wustite.

In actual practice the rates observed are about one-half the values calculated from the known data.

Many generalized forms of rate equations of various levels of complexity (Ref. 7-9) have been derived for gaseous reduction of iron oxide particles. If we note that even for a simple limiting case as that shown here the interpretation of the rate data is far from rigorous, it pays not to over-emphasise the utility of complex mathematical formulations.

THERMODYNAMICS OF SLAG-METAL REACTIONS

There are three reaction equilibria which are of primary importance in the Blast Furnace Hearth representing silicon, manganese and sulphur reactions:-

$$(SiO_2) + 2\underline{C} = \underline{Si} + 2CO \tag{10}$$

$$(MnO) + \underline{C} = \underline{Mn} + CO \tag{11}$$

$$(CaO) + \underline{S} + \underline{C} = (CaS) + CO \tag{12}$$

where the brackets represent constituents dissolved in the slag and the underline indicates elements dissolved in iron.

The equilibrium distribution of silicon, manganese and sulphur between carbon-saturated liquid iron and blast furnace type slag containing CaO, MgO, Al_2O_3 and SiO_2 are shown in Figures 5, 6 and 7 and represent the results of many investigations (Ref. 10).

The importance of coupled reactions in complex slag-metal equilibrium situations was first pointed out by Oelsen and co-workers (Ref. 11 & 12). They showed that reactions involving three phases will approach equilibrium only slowly in a dynamic system like the blast furnace. Therefore it seems likely that reactions involving only slag and metal will proceed more rapidly and coupled reactions should be considered. For example the manganese and silicon reactions may be written

$$2 (MnO) + \underline{Si} = (SiO_2) + 2 \underline{Mn} \tag{13}$$

From the experimental data of Oelsen et al the equilibrium constant for this reaction may be given as

$$\log \left\{ \frac{[\%Mn]}{(\%MnO)} \right\}^2 \frac{(\%SiO_2)}{\%Si} = 2.79\ B - 1.16 \tag{14}$$

where B represents the basicity of the slag $\frac{\%CaO + \%MgO}{\%SiO_2}$.
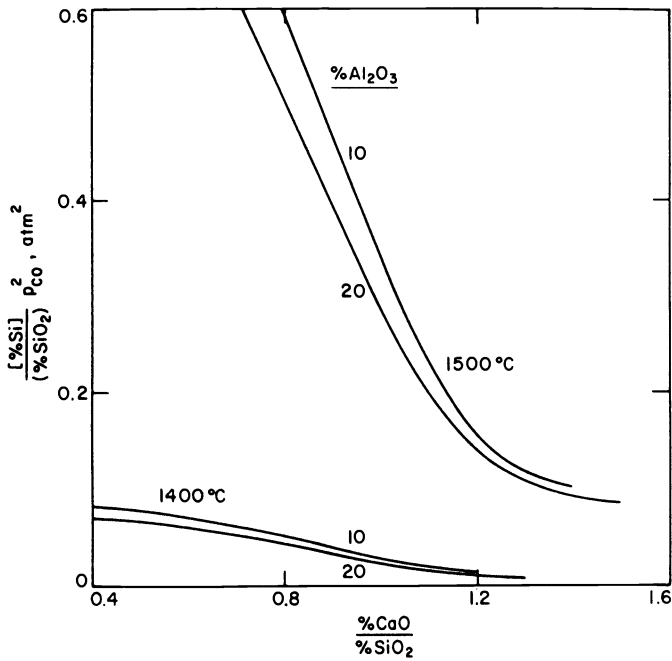

Fig. 5. Equilibrium distribution of silicon between metal and slag as a function of slag basicity.
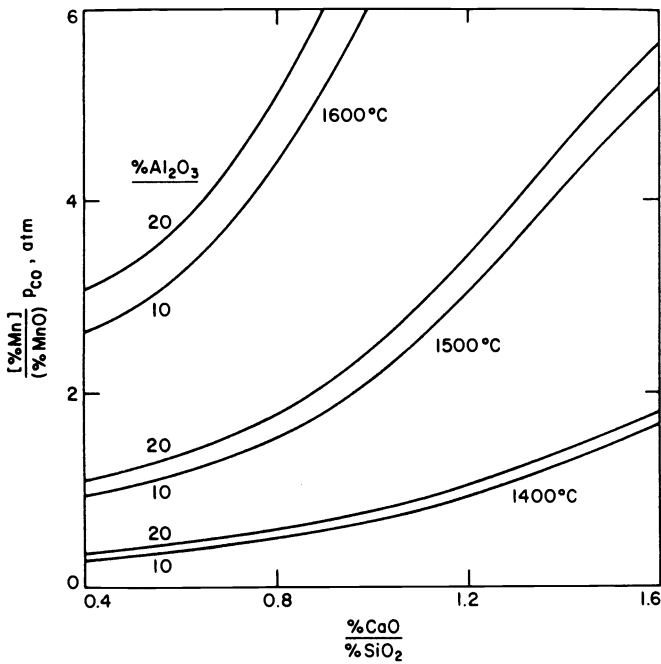

Fig. 6. Equilibrium distribution of manganese between metal and slag as a function of slag basicity.
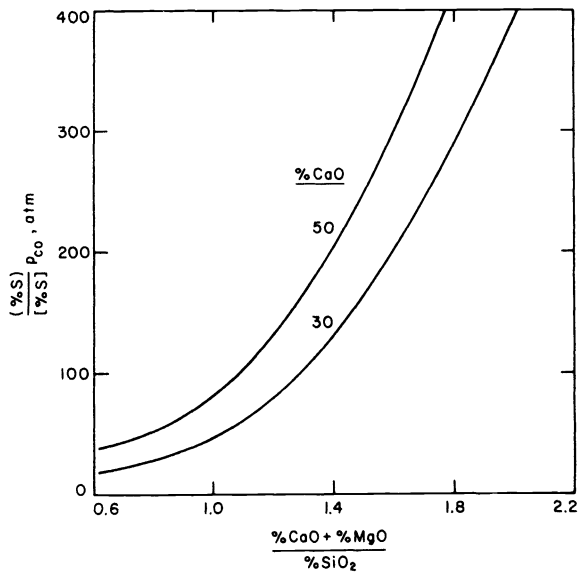
Fig. 7. Equilibrium distribution of sulphur between slag and metal as a
         function of slag basicity at 1500°C.

It is interesting to note that the effect of temperature on this relationship is virtually
negligible.

Most slag-metal reactions are electrochemical in nature, thus sulphur transfer from metal to
slag requires electrons and is accompanied by the oxidation of a dissolved element such as
manganese and silicon. Thus, the sulphur reaction involving manganese is represented by the
equation

$$(CaO) + \underline{Mn} + \underline{S} = (CaS) + (MnO) \tag{15}$$

Once again we can use the data of Oelsen et al to formulate the necessary equilibrium
relationship,

$$\log \frac{(\%S)}{[\%\underline{S}]} \frac{(\%MnO)}{[\%\underline{Mn}]} = \frac{9080}{T} - 5.83 + \log (\%CaO) \tag{16}$$

In a similar manner, we can write the sulphur-silicon reaction:

$$(CaO) + \tfrac{1}{2}\underline{Si} + \underline{S} = (CaS) + (\tfrac{1}{2}SiO_2) \tag{17}$$
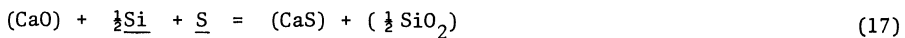
where the following equilibrium relationship can be applied

$$\log \frac{(\%S)}{[\%\underline{S}]} \frac{(\%SiO_2)}{[\%\underline{Si}]}^{\tfrac{1}{2}} = \frac{9080}{T} - 6.38 + \log (\%CaO) + 1.395B \tag{18}$$

It is interesting to note how actual blast furnace data agree with these equilibrium predic-
tions. In typical blast furnace practice, the distribution ratios for manganese, silicon
and sulphur usually lie in the following ranges

$$[\underline{Mn}] / (MnO) = 0.6 - 4, \quad [\underline{Si}] / (SiO_2) = 0.15 \text{ to } 0.08 \text{ and } (S)/[S] = 20\text{-}120$$

Comparison of these ratios with the equilibrium data indicate that the values are several
fold lower than the equilibrium values for three phase equilibria. In other words, these
reactions do not achieve equilibrium in the blast furnace.

If we consider blast furnace data in comparison with the slag-metal equilibrium, it can be
seen that even the two phase manganese-silicon and silicon-sulphur equilibria are not
reached. However, there is a trend for the product of the silicon and manganese ratios to

increase with increasing slag basicity. For all blast furnaces, the data lie below the equilibrium line indicating that the metal-slag reaction proceeds in the direction

$$2(MnO) + \underline{Si} \rightarrow 2\underline{Mn} + (SiO_2)$$
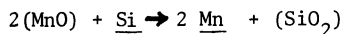
These results indicate that the final silicon level in the metal is determined by this oxidation reaction and not by the carbon reduction reaction which was previously supposed.

For sulphur reaction, disagreement with three phase equilibria is again noted from plant data. However a comparison of sulphur and manganese distribution data indicate that for many blast furnaces, the sulphur-manganese reaction is close to equilibrium. Once again it is interesting to note that if the silicon-manganese reaction had achieved equilibrium, the [Mn]/(MnO) ratio would have been greater and because of the approach to equilibrium of the sulphur-manganese reaction, more desulphurisation would have occurred. In practical terms, the greater the rate of reaction by higher temperature or higher MnO content of the slag, the greater will be the desulphurisation of the hot metal.

OXYGEN STEELMAKING REACTIONS

For several years oxygen steelmaking was limited to top blowing of oxygen through a lance with a converter. The reason was that use of a bottom tuyere as in the old Bessemer process was limited because of the excessive wear of the vessel base due to the high temperatures generated by the oxidation reactions. However a tuyere arrangement was developed by Eisenwerk Gesellschaft Maximillianshutte, MbH West Germany in co-operation with Air Liquide of Canada which significantly improves the base refractory life and led to the introduction of the bottom-blown oxygen process. The tuyere consists of an oxygen-blowing pipe encased within a slightly larger pipe. When a hydro-carbon, such as natural gas, is blown through the annulus between the two pipes, the endothermic decomposition of the hydrocarbon at the mouth of the tuyere effectively cools the tuyere and allows the introduction of pure oxygen without excessive refractory erosion. Another unique feature of the bottom blown process is that powdered burnt lime may be blown together with oxygen, allowing phosphorus to be removed during decarburisation.

Whether top or bottom blowing is used, the chemical reactions are fast and the rate of refining is controlled primarily by diffusional and convective mass-transport processes.

Typical examples of the process of oxidation of carbon, phosphorus, silicon and manganese in top and bottom blown processes are shown in Figure 8 and 9.
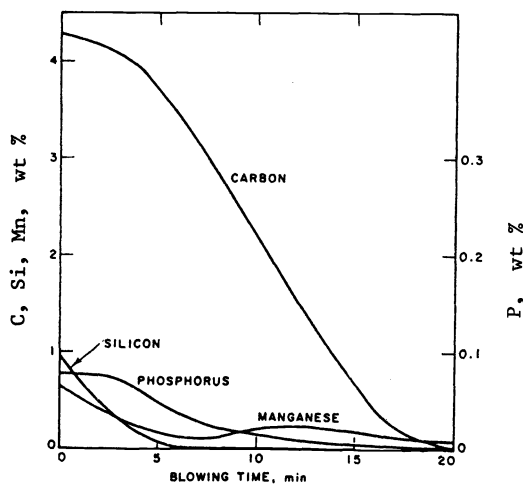

Fig. 8. Oxidation of **carbon**, phosphorus, silicon and manganese during top-blown **steelmaking**.
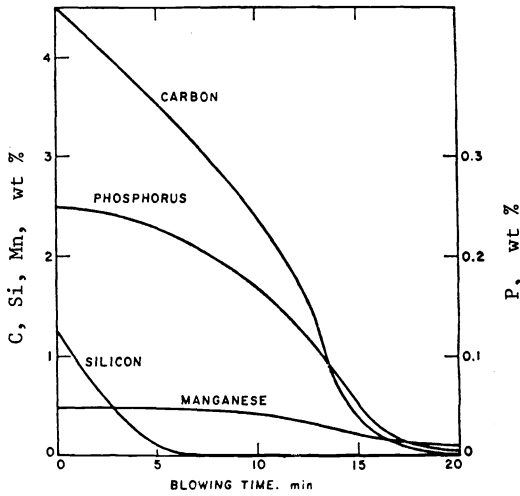
Fig. 9. Oxidation of carbon, phosphorus, silicon and manganese during
         bottom-blown steelmaking.

In both cases, the carbon, silicon and phosphorus curves have similar shapes.

There is a marked difference, however, in the oxidation of manganese. In the bottom-blown
process, Q-BOP process, with lime injection, there is hardly any manganese oxidation until
nearly all the silicon is removed. In comparison, in the top-blown or BOP process, manganese
and silicon are oxidised simultaneously and after silicon removal, manganese reversion occurs
to the metal. The significance of this reversion becomes of significant interest when
departures from slag-metal equilibrium are considered.

The slag-metal manganese reaction may be represented as

$$\underline{Mn} + (FeO) = (MnO) + \underline{Fe} \tag{19}$$

with an equilibrium parameter K_{Mn} given by

$$K_{Mn} = \frac{(\%MnO)}{[\%\underline{Mn}]\,(\%FeO)} \tag{20}$$

which decreases with increasing basicity of the slag because of the variation of the activity
coefficient ratio of the oxides, $\gamma_{MnO}/\gamma_{FeO}$ with composition. Values of K_{Mn} are calculated
for samples taken from an actual blow are plotted against slag basicity see Figure 10.
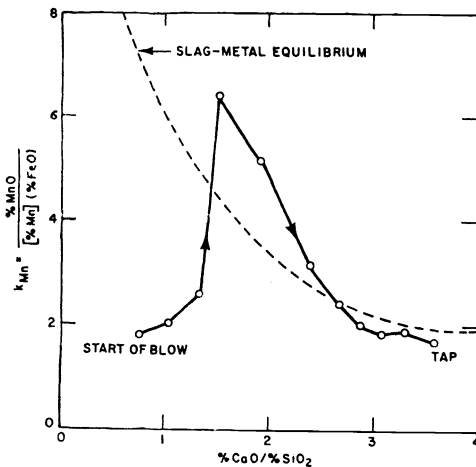

Fig. 10. Changes in slag-metal distribution during top-blown steelmaking

The dotted curve is calculated from the known slag-metal equilibrium data. It should be noted that after the first few minutes of the blow the values of K_{Mn} lie above the equilibrium curve. As the slag basicity increases with the progress of the blow and more lime dissolves, the value of K_{Mn} approaches that for slag-metal equilibrium. This behaviour is not observed in bottom blowing of oxygen and lime, where during the initial stages of the blow, the manganese in the metal remains essentially unchanged and well above the equilibrium value. It should be noted that final manganese contents of steel at tap in Q-BOP heats are usually a little higher than those obtained in other steelmaking practice.

DEOXIDATION AND DESULPHURISATION OF STEEL

Because of the small solubility of oxygen in solid steel, liquid steel must be deoxidised to a low level to provide sound cast metal. The choice of deoxidant depends on the required levels of residual oxygen in the final steel. Because of its tremendous importance, a large quantity of deoxidation equilibrium information is available related to all the common de;-oxidation metals. Some of the latest information is summarised in Figure 11. as a log-log
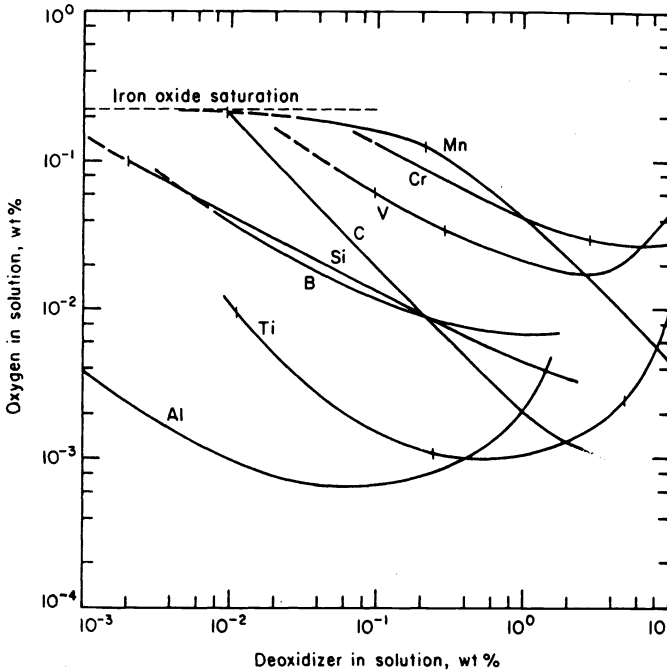

Fig. 11. Deoxidation equilibria in liquid iron alloys at 1600°C.

graph of the concentration of oxygen in liquid steel against the concentration of added oxidant. In all cases, oxygen and alloying element in solution are in equilibrium with the appropriate gas, liquid or oxide phase at 1600°C.

The solubility of the deoxidation product in liquid steel is represented by

$$M_x O_y = x \underline{M} + y \underline{O} \qquad (21)$$

where $\quad K = \dfrac{[a_{\underline{M}}]^x \, [a_{\underline{O}}]^y}{a_{M_x O_y}} \qquad (22)$

For convenience the solute activities are chosen such that at infinitely dilute solutions $a_i = $ wt% i in the metal. Inserting the activity coefficients, $f_i = a_i / $wt% i the solubility product for unit activity of the oxide is

$$K = [\% \underline{M}]^x \, [\% \underline{O}]^y \cdot f_M^x \cdot f_O^y \qquad (23)$$

where f_M, f_O approach unity when %M approaches zero.

For the alloys considered, f_M increases with increasing concentration if solute M; however, f_O decreases with increasing %M. The result is that a minimum may occur in the oxygen solubility at a particular solute concentration. The greater the stability of the deoxidation product, the lower is the concentration of the solute at which the oxygen solubility reaches a minimum.
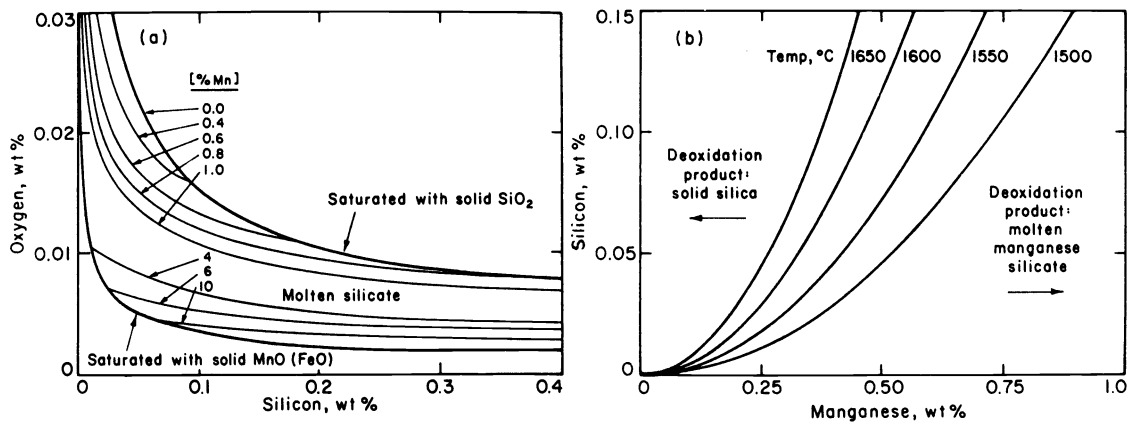
Fig. 12. Equilibrium relationship for deoxidation of steel with silicon
and manganese at 1600°C.

Although a perusal of the deoxidation equilibria indicates that silicon is a better deoxi-
dant that manganese, simultaneous deoxidation by these two elements gives lower residual
oxygen in solution because of the reduced silica activity. The equilibrium data for
simultaneous deoxidation of steel by silicon and manganese at 1600°C are given in Figure 12.

It can be seen that with both deoxidants present the deoxidation product is a molten manga-
nese silicate rather than solid silica. The molten silicate exhibits an activity of silica
lower than pure silica and consequently, for a given silicon content of the steel, the
residual oxygen is less than that obtained in the presence of solid silica.

Although there are many variations in the methods of desulphurisation of steel, one unique
feature is the necessity for effective deoxidation of the steel. All desulphurising elements
also react with oxygen in the metal, therefore the overall reaction which must be considered
is that involving both an oxide and a sulphide phase.

$$\underline{S} + MO = \underline{O} + MS \tag{24}$$

For the case of pure oxide and sulphide formation, the equilibrium constant is given by the
ratio of the activities of oxygen and sulphur in the liquid steel. Thus, consideration of
the alkaline earth elements indicates that magnesium is a poor desulphurising agent in steel
and improved desulphurisation is obtained with calcium and barium. The usual practice in
ladle desulphurisation is to inject alloys of calcium with argon deep into the steel melt
after aluminium deoxidation. The success of good ladle desulphurisation depends on the
precautions taken to avoid oxygen pick up from the air, slag and refractory linings of the
ladles.

Whereas it has been impossible to give a complete coverage of the subject in this short
communication, I hope that it has provided a brief outline of the importance of physical
chemistry in metal production and the part it has played in metallurgical development.

REFERENCES

1. P. Reichardt, Arch. Eisenhuttenw . 1, 77-101 (1927/28).
2. A. Rist and G. Bonnivard, Rev. Met. 60, 23-38 (1963).
3. A. Rist and N. Meysson, Rev. Met. 61, 121-46 (1964).
4. L. Von Bogdandy and H.J.Engell, The reduction of iron ores, Springer-Verlag Berlin-
    Heidelberg, New York (1971).
5. E.T. Turkdogan and J.V. Vinters, Met. Trans. 3, 1561-74 (1972).
6. E.T. Turkdogan and J.V. Vinters, Met. Trans. 2, 3175-88 (1971).
7. R.H. Spitzer, F.S. Manning and W.O. Philbrook, Trans. Met. Soc. AIME, 236, 726-42,
    (1966).
8. R.H. Tien and E.T. Turkdogan, Met. Trans. 3, 2039-48 (1972).
9. J. Szekely, J.W. Evans and H.Y. Sohn, Gas-solid reactions, Academic Press, New York,
    (1976).
10. E.T. Turkdogan, Met. Trans. B 9B, 163-79 (1978).
11. W. Oelsen and H.G. Schubert, Arch. Eisenhuttenw 35, 1039-57, 1115-22, (1964).
12. W. Oelsen, H.G. Schubert and O. Oelsen, Arch. Eisenhuttenw 36, 779-90, (1965).